Available online at www.sciencedirect.com

ScienceDirect

Physics Procedia 83 (2016) 808 – 817

Physics Procedia

9th International Conference on Photonic Technologies - LANE 2016

Weldability of additive manufactured stainless steel

Ville-Pekka Matilainen[a,*], Joonas Pekkarinen[a,b], Antti Salminen[a,b]

[a]*Lappeenranta University of Technology, Tuotantokatu 2, Lappeenranta 53850, Finland*
[b]*Machine Technology Center Turku Ltd., Lemminkäisenkatu 28, Turku 20520, Finland*

Abstract

Part size in additive manufacturing is limited by the size of building area of AM equipment. Occasionally, larger constructions that AM machines are able to produce, are needed, and this creates demand for welding AM parts together. However there is very little information on welding of additive manufactured stainless steels. The aim of this study was to investigate the weldability aspects of AM material. In this study, comparison of the bead on plate welds between AM parts and sheet metal parts is done.

Used material was 316L stainless steel, AM and sheet metal, and parts were welded with laser welding. Weld quality was evaluated visually from macroscopic images. Results show that there are certain differences in the welds in AM parts compared to the welds in sheet metal parts. Differences were found in penetration depths and in type of welding defects. Nevertheless, this study presents that laser welding is suitable process for welding AM parts.

Peer-review under responsibility of the Bayerisches Laserzentrum GmbH

Keywords: Additive manufacturing; laser welding; weldability; stainless steel

1. Introduction

Additive manufacturing is technology which enables creation of innovative and complex parts with good mechanical properties. These innovative geometries like deep helical cavities, integrated cooling channels and parts with unique design for the demanded applications are easy to produce. However, the part size in additive manufacturing, especially in powder bed fusion (PBF) technique, is usually relatively small. Joining of AM parts together or to existence construction is a way to overcome the part size limitation (Casalino et al. 2013). Joining of

* Corresponding author. Tel.: +35-8401524034 .
E-mail address: ville-pekka.matilainen@lut.fi

Peer-review under responsibility of the Bayerisches Laserzentrum GmbH
doi:10.1016/j.phpro.2016.08.083

AM parts by laser welding is area of where very small amount of research have been published. It is commonly known that most materials that can be welded can be used in PBF process to build parts (Laitinen, 2014 & Järvinen, 2015). It is also known that PBF produced parts are almost porosity free, so this could indicate that PBF parts can be welded with laser welding (Yasa, Kruth, 2011). In principle PBF process is laser welding but in very small scale, so also this indicates that laser welding could be good method for joining AM parts together. (Tolosa et al. 2010)

Laser welding is an industrial joining process and used as an alternative to conventional arc welding processes nowadays. The advantages of laser welding are high welding speed, which enables low heat input, and deep and narrow weld with small HAZ (heat affected zone) (Lippold & Kotecki 2005). Laser welding can be executed as conduction limited welding or keyhole welding. In keyhole welding laser beam absorbs to the welded material surface, the material heats, melts and starts to boil. This boiling effect, in case of stainless steels, causes metal vapour cavity, a keyhole, mainly from the vapours from iron, nickel and chromium. When the welding head is moving, molten material flows around the keyhole, solidifies and forms the weld (Vänskä, 2014).

Nomenclature

AM	additive manufacturing	CCD	charge coupled device
PBF	powder bed fusion	ρ	material density [kg/ mm^3]
HAZ	heat affected zone	V_{WM}	weld metal volume [mm^3/s]
CR	cold rolled	c	specific heat of fusion [J/kgK]
Yb	ytterbium	T_m	melting temperature [K]
W	watt	T_0	room temperature [K]
°C	degrees in celsius	L	latent heat of melting [J/kg]

2. Experimental procedure

2.1. Geometry of the test pieces

The dimensions of the welding test specimen were approx. 50 mm x 100 mm x 3 mm for test pieces made out of cold rolled 316L and PBF manufactured 316L stainless steel sheets. In PBF sheets, the welding was performed in building direction. Dimensions of the test pieces and build direction of PBF test piece are shown in Fig. 1.

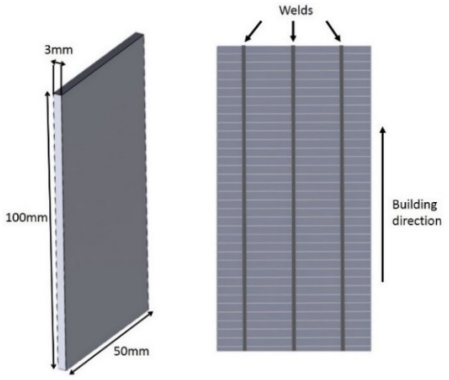

Fig. 1. Left: dimensions of the test pieces, Right: building and welding direction of PBF test pieces.

2.2. Materials used in this study

Two stainless steel 316L materials was used in the study. PBF sheets were manufactured from Höganäs Stainless Steel 316L powder and cold rolled (CR) stainless steel plates were Outokumpu 1.4404 (316L). Elementary analysis

were performed for both materials and the chemical compositions of the materials are presented in tables 1 and 2. Elemental analysis were made with Bruker Q4 Tasman, which is CCD based optical emission spectrometer for the metal analysis. The analysis measurements were taken from the surface of the CR and PBF plates from three separate places and then averaged.

Table 1. Höganäs 316L chemical composition, analyzed with Bruker Q4 Tasman.

Cr [%]	Ni [%]	Mo [%]	Mn [%]	Si [%]	Cu [%]	C [%]	P [%]	S [%]	Fe [%]
18.89	7.54	2.65	1.56	0.55	0.05	0.019	0.014	0.150	Balance

Table 2. Cold rolled Outokumpu 1.4404 (316L) chemical composition, analyzed with Bruker Q4 Tasman.

Cr [%]	Ni [%]	Mo [%]	Mn [%]	Si [%]	Cu [%]	C [%]	P [%]	S [%]	Fe [%]
18.71	6.38	2.16	1.91	0.40	0.39	0.030	0.027	0.150	Balance

2.3. PBF sheet fabrication

PBF sheets were manufactured with modified research PBF system, similar to EOS EOSINT M270. This system has 200 W Yb-fiber laser. Focal point of the laser beam was 100µm and the build volume of this system is 245 mm x 245 mm x 215 mm. Manufacturing of the sheets was executed as one build. Nitrogen served as shielding gas in the process chamber. The manufacturing parameters are shown in table 3.

Table 3. PBF manufacturing parameters.

Laser Power [W]	Laser scan velocity [mm/s]	Layer thickness [µm]	Hatch distance [mm]
200	1000	20	0.1

The scanning direction was altered in every layer to achieve full dense structure. After the manufacturing the sheets were sawed off from the building platform and sawed to the test specimen dimensions. No other post processing was made.

2.4. Bead on plate laser welding of the test pieces.

Laser welding was performed with IPG YLS-10000 fiber laser which has maximum power of 10 kW. Precitec YW50 welding head was used with 300 mm focal length focusing lense, 150 mm collimator lense. Two different fiber dieameters were used 200µm and 600µm. No shielding gas was used. The welding setup is presented in Fig. 2.

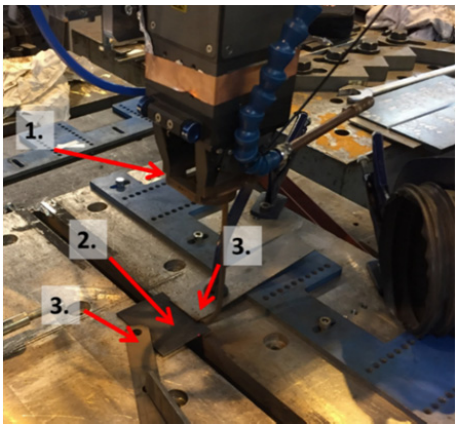

Fig. 2. Laser welding setup; 1. laser welding head, 2. test piece, 3. clamping of the test piece.

2.5. Laser welding parameters

For all welding tests, the focal point position was set on top of the test pieces. Welds were bead on plate welds. Three welds with same parameters were welded into each test piece and the test pieces were cooled down after each weld by blowing compressed air on them. All welds were done in room temperature (22 °C). Parameters which were varied for the experiments were laser power, welding speed and diameter of optical fiber. Laser welding parameters are presented in table 4.

Table 4. Laser welding parameters.

Test No.	Laser Power [kW]	Welding speed [mm/min]	Optical fiber diameter [µm]	Energy input [J/mm]
1	1.5	1500	200	60
2	2	1500	200	80
3	2.5	1500	200	100
4	1.5	1750	200	51
5	2	1750	200	69
6	2.5	1750	200	86
7	1.5	2000	200	45
8	2	2000	200	60
9	2.5	2000	200	75
10	3	1500	600	120
11	3.5	1500	600	140
12	4	1500	600	160
13	3	1750	600	103
14	3.5	1750	600	120
15	4	1750	600	137
16	3	2000	600	90
17	3.5	2000	600	105
18	4	2000	600	120

The energy input of laser welding was calculated by using following equation:

$$E = \frac{P}{v} \tag{1}$$

where E is the energy input (J/mm), P is the laser power (W) and v is the welding speed (mm/s) (Dahotre & Harimkar, 2008).

2.6. Analysis methods

Once test pieces were welded, the top and root surfaces of the test pieces were photographed. The section for macroscopic analysis was sawed off from the middle of the test piece. The sections were then polished and electro etched with 10% oxalic acid. The current and voltage for electro etching was 30 V and 2 A, respectively. The etching time was 45 seconds. Weld beads from the polished sections were macro photographed and weld widths and areas were measured. Quality of the welds were evaluated using the ISO 13919-1 standard: Electron and laser beam welded joints. Guidance on quality levels for imperfections, Part 1: Steel (ISO 1319-1 standard).

3. Results and discussion

3.1. Weld geometry and quality

Quality of the welds varied between the materials that were welded. Visual inspection of the surfaces of the welds showed that when cold rolled 316L was weld with fiber diameter of 200 µm, there were large amount of spattering, especially when laser power was highest (2.5 kW). With PBF manufactured 316L sheets no similar spattering was noticed (see Fig. 3). When 600 µm optical fiber was used for welding, similar spattering was not noticed.

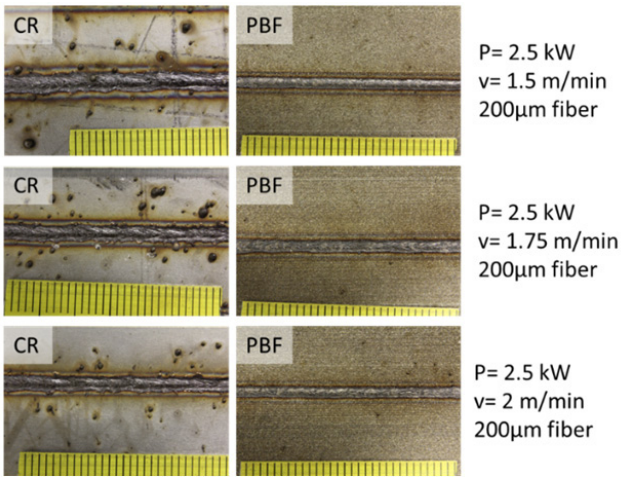

Fig. 3. Spattering on CR316L welds. No similar effect on PBF welds.

The PBF material was more prone to cracking from the weld centerline when laser power of 4 kW and welding speeds 1.5 m/min and 1.75 m/min were used. Only imperfections that were found were cracking and lack of penetration, imperfections 1 and 8a , according the ISO 13919-1 standard. All welds without cracks passed the visual inspection when the classification of the welds were in class D (moderate). Cracking of the welds were found

only in PBF material. All welds without cracks or lack of penetration were classified as class B (stringent) according to the ISO 13919-1. Fig. 4 shows examples of imperfections found.

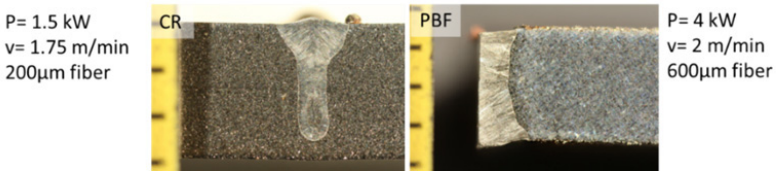

Fig. 4. Examples of imperfections of the welds. Left: Cold rolled 316L, lack of penetration, right: PBF 316L cracked weld.

The shape of the cross sections of the welds varied between the welded materials especially when welding was done with 200 µm optical fiber. In PBF welds, the cross-section of the welds were more straight than welds in cold rolled material. Fig. 5 shows different shapes of welds made with same parameters.

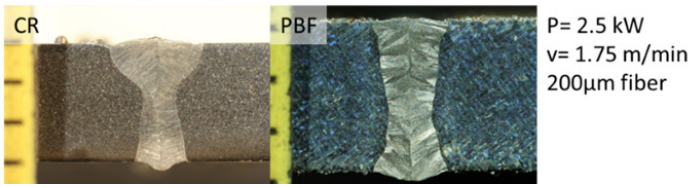

Fig. 5. Different weld shapes in CR= cold rolled 316L stainless steel and PBF= powder bed fusion 316L stainless steel. Both welds made with same parameters.

As it can be seen from Fig.5, the shape of the weld in CR material is beaker shaped, while the weld in PBF material is more straight shaped. The difference in weld shapes can be as a result of different absorption properties between the surfaces of the materials. Bergström (Bergström, 2005) researched the absorptance of Nd:YLF and Nd:YAG laser lights into the steels at room temperature. In this research the cold rolled stainless steel had absorption of 37% of Nd:YLF laser light(Bergström, 2005). Since the surface of the PBF material is much rougher and more matte than on CR material it can be assumed that the absorption rate is higher and therefore the keyhole can be formed more easily to the material and more straight shaped and fully penetrated welds can be created even with lower laser power.

Many of welds in CR 316L material were wider than ones in PBF material. With both welded materials, some cross-sections of the welds looked like they had been welded from both sides, although this was not the case. This phenomena could be explained with different keyhole modes. The keyhole modes in high power laser welding was investigated by Vänskä (2014) in his doctoral thesis. In Vänskäs studies some of the welds had “twin top” geometry where the root side of the weld has same features that the top side, slightly larger surface width and similar solidification lines. This behavior was explained so that the keyholes front wall angle was small, and reflectivity was large, which led redirection of the laser light to deeper into the material and eventually out of the root side. He called this keyhole mode as kaleidoscope keyhole. This kaleidoscope keyhole mode leads into the “twin top” geometry (Vänskä, 2014). Fig. 6 presents the “twin top” weld phenomena and one of the “twin top” welds that were acquired in the welding tests. This twintop weld geometry was shown in both PBF welds and in CR welds.

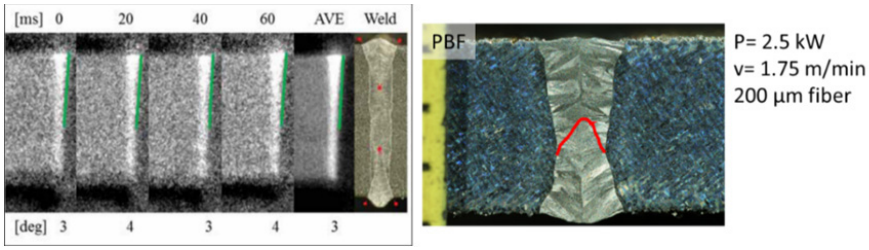

Fig. 6. Left: kaleidoscope keyhole mode and "twin top" weld geometry (Vänskä 2014). Right: one of twin top welds acquired during the welding tests. Red line describes the shape of the weld from the root side.

3.2. Analysis of weld cross-section geometry

The width, depth and area of the weld cross-section were measured from the macro images by using ImageJ software. Like mentioned before, the shape of the welds differed between these two materials and the welds were wider in cold rolled material when averaged. The weld widths were measured from the top of the welds, close from the surface. Fig. 7 presents the weld widths when 200 µm optical fiber was used.

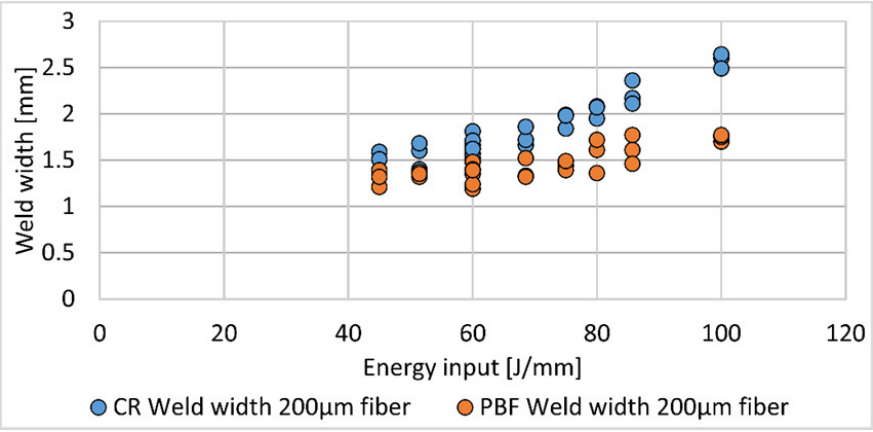

Fig. 7. Energy input vs. weld width when welding was done with 200 µm optical fiber.

As it can be seen from the Fig. 7, the weld width was wider in cold rolled welds. However, the weld shape was usually more beaker shaped, as shown in Fig. 5., so the welds in CR material narrowed to the root, when the PBF welds were more straight, and even X shaped. The penetration depth differed also between the welds in these materials. In cold rolled material, welds 1, 4, and 7, were only partially penetrated, whereas only weld 7 in PBF material was partly penetrated. The other welds welded with 200 µm fiber were full penetrated. Welds with low energy input were also prone to have pores in the weld. Especially in PBF material. Table 5 presents the penetration depths of the welded materials.

Table 5. Penetration depths of the welded materials, when 200 µm optical fiber was used.

Material	Weld 1	Weld 2	Weld 3	Weld 4	Weld 5	Weld 6	Weld 7	Weld 8	Weld 9
CR 316L	2.77 mm	Full	Full	2.56 mm	Full	Full	2.37 mm	Full	Full
PBF 316L	Full/Pores	Full	Full	Full/Pore	Full	Full	2.55 mm/Pore	Full	Full

The width of the welds were similarly measured from the welds made with 600 µm optical fiber. The energy input vs. the weld width is presented in Fig. 8.

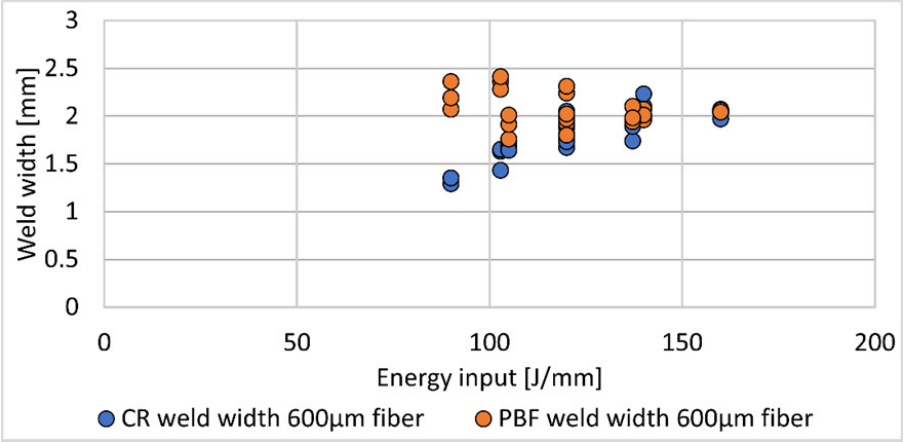

Fig. 8. Energy input vs. weld width, when welding was done with 600 µm optical fiber.

As it can be observed from Fig. 8, the welds were wider in PBF material when energy input was lower, less than 120 J/mm when 600 µm fiber was used. Otherwise the widths were close to each others. With these energy inputs only one of the welds (weld No. 16, energy input of 90 J/mm) was not fully penetrated in both materials. With higher energy inputs, 120 J/mm and above, PBF welds had tendency to crack slightly or completely from the middle of the weld. This may be caused by possible residual stresses in PBF material. However, it needs further studies.

3.3. Welding efficiency

Since the welding of additive manufactured parts is not yet very widely researched field, it was decided to see if there is differences in the welding efficiency between PBF manufactured stainless steel and cold rolled stainless steel. This comparison was done by measuring the areas of the weld cross-sections and from there calculated the needed energy to melt the specific amount of material. Melting efficiency can be calculated by dividing the energy used for melting the material by the total energy input. According to Swift-Hook and Lampa et al., (Swift.-Hook, 1973, Lampa et al., 1995) the maximum melting efficiency for laser welding is approx. 50%. The needed melting energy can be calculated by Equation 2.

$$P = \rho * V_{WM} * (c * (T_m - T_0) + L) \quad (2)$$

where,

P = laser power [W]
ρ = material density [kg/mm^3]
V_{WM} = weld metal volume [mm^3/s]
c = specific heat of fusion [J/kgK]
T_m = melting temperature [K]
T_0 = room temperature [K]
L = latent heat of melting [J/kg]

When replacing the weld metal volume (V_{WM}) with welding speed v (mm/s) multiplied by the weld cross-section area A_{WM} (mm^2) the equation can be rewritten as follows:

$$P = \rho * v * A_{WM} * (c * (T_m - T_0) + L) \quad (3)$$

The melted areas were measured and in average the melted area was larger in cold rolled stainless steel than in powder bed fusion manufactured stainless steel. Fig. 9 presents the weld cross-section area vs. energy input.

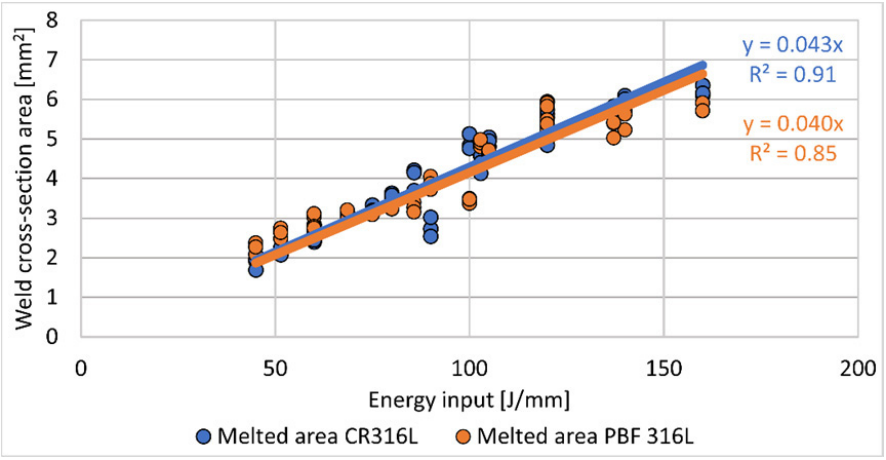

Fig. 9. Weld cross-section area vs. energy input.

As it can be observed from the Fig. 9 there is only small differences in the size of the melted cross-section area between the two materials. It seems that with lower heat inputs (80 J/mm or less) the PBF material is melted more efficiently than the cold rolled. The reason for this is that the welds were fully penetrated with lower energy inputs in PBF material and therefore the area of weld cross-section was larger. When the energy inputs were higher, the larger melted areas were in cold rolled material.

The power needed to melt specific cross-section area was calculated by equation 3, and the results can be seen from Fig. 10.

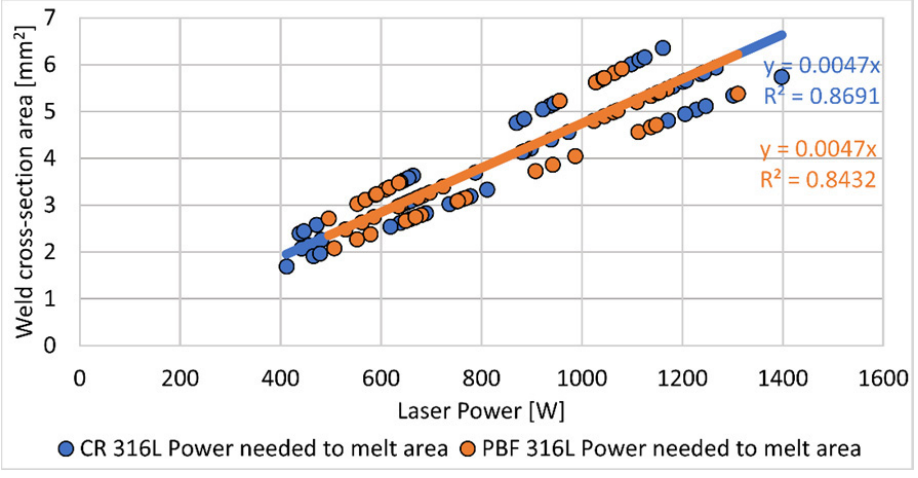

Fig. 10. Calculated need of laser power to melt the cross-section area.

As it can be seen from Fig. 10, there is no large variations between the two materials in case of melting efficiency. It can be seen that the calculated melting energy is in both cases much lower than actual power which was used in welding. Actually the melting efficiency was with cold rolled material 31.51 % and for the PBF material just a slightly higher 31.65 %.

4. Conclusions

Effect of energy input in laser welding on weldability, weld quality and weld geometry of welds between powder bed fusion (PBF) fabricated stainless steel 316L parts and cold rolled (CR) sheet metal 316L parts were studied by bead on plate welds. Tested parameters were optical fiber diameter, laser power and welding speed.

It was concluded in this study that in general PBF manufactured parts can be welded with good quality. All produced welds were visually inspected and evaluated according the ISO standard: ISO 13919-1 Electron and laser beam welded joints. Guidance on quality levels for imperfections, Part 1: Steel. All welds without cracks or lack of penetration were evaluated to the B class (stringent). All the welds without cracks were classified into C (intermediate) class. Cracking was present only in welds in PBF material.

This study showed that laser welding of PBF stainless steel differs slightly from CR stainless steel welding. When energy input is low, full penetration welds can be achieved easier into PBF material. However, when the weld lacked penetration, large pores were found in welds of PBF material. Increase of the energy input is effecting on the tendency of weld cracking in PBF material. The cracking might be present because of possible residual stresses in PBF material. However, this needs further studies. Energy input of the welding is to be considered as critical factor for welding of PBF fabricated stainless steel 316L components.

Melting efficiency was also studied and calculated. The measurements showed that with lower energy inputs (80 J/mm or less) the PBF melts more efficiently than CR material. When energy input is higher (90 J/mm or more) the CR material melted more efficiently and the melted area cross-section was larger. However, with both materials the melting efficiency was quite low, 31.51 % and 31.65 % for CR and PBF materials respectively. It was concluded that laser welding melts both materials (CR 316L and PBF 316L) almost equal amounts, but the difference in weld shape formation needs further studies.

Acknowledgements

This study was carried out as a part of the Finnish Metals and Engineering Competence Cluster (FIMECC) program MANU - Future Digital Manufacturing Technologies and Systems, P6 Next Generation Manufacturing. Authors express their gratitude to LUT Laser personnel and to LUT metallurgy lab personnel for the help of executing the experimental testing.

References

Bergström, D., 2005. “The Absorptance of Metallic Alloys to Nd:YAG and Nd:YLF Laser Light” Licentiate Thesis, Luleå University of Technology.

Casalino, G., Campanelli, S. L., Ludovico, A. D., 2013. “Laser-arc hybrid welding of wrought to selective laser molten stainless steel,” International Journal of Advanced Manufacturing Technology, Issue 68, pp 209-216.

Dahotre, N. B. & Harimkar, S. P., “Laser Fabrication and Machining of Materials,” Springer Science + Business Media, LCC. New York. (2008) 558 p.

Järvinen, J-P., “Welding of additively manufactured stainless steel parts: Comparative study between sheet metal and selective laser melted parts,” 2014. Master’s thesis, Lappeenranta University of Technology, 65p.

Laitinen, V., “Weldability of powder bed fusion fabricated stainless steel 316L metal sheets to cold rolled sheet metal, 2015. ” Master’s thesis, Lappeenranta University of Technology, 66 p.

Lampa, C., Powell, J., Ivarson, A. and Magnusson, C. 1995A. “Factors affecting efficiency of laser welding.” Lasers in Engineering, Vol., No:4, pp.73-83.

Lippold, J. C. & Kotecki, D. J. 2005. ”Welding Metallurgy and Weldability of Stainless Steels”. John Wiley & Sons, Inc., New Jersey. 357 p.

Swift-Hook, D.T. and Gick, A.E.F. 1973. “Penetration welding with lasers”. Welding Journal, 52, 11, pp. 492s-499s.

Tolosa, I., Garciandía, F., Zubiri, F., Zapirain, F., Esnaola, A., 2010. “Study of mechanical properties of AISI 316L stainless steel processed by selective laser melting, following different manufacturing strategies,” International Journal of Advanced Manufacturing Technology, 51, pp.639-647.

Vänskä, M., 2014.” Defining the keyhole modes – the effects on the weld geometry and the molten pool behaviour in high power laser welding of stainless steels,” Doctoral Thesis, Lappeenranta University of Technology, Acta Universitatis Lappeenrantaensis 625 112 p.

Yasa, E., Kruth, J-P., 2011. ”Microstructural investigation of selective laser melting 316L stainless steel parts exposed to laser re-melting,” Procedia Engineering, 19, pp.389-395.